1-to-$(N \times N)$ optical fan-out module for optical interconnects

1997 J. Opt. 28 70

(http://iopscience.iop.org/0150-536X/28/2/003)

J. Opt. **28** (1997) 70–73. Printed in the UK PII: S0150-536X(97)82277-0

1-to-($N \times N$) optical fan-out module for optical interconnects

Der-Chin Su†, Jen-Tsorng Chang† and Yang-Tung Huang‡

† Institute of Electro-Optical Engineering, National Chiao-Tung University, 1001 Ta-Hsueh Road, HsinChu, 30050, Taiwan, Republic of China
‡ Department of Electronics Engineering and Institute of Electronics, National Chiao-Tung University, 1001 Ta-Hsueh Road, HsinChu, 30050, Taiwan, Republic of China

Received 10 September 1996, accepted 5 February 1997

Abstract. Based on the structure of substrate-mode holograms, a new type of 1-to-($N \times N$) optical fan-out module which consists of two layers of grating arrays for optical interconnects is presented. The first and second layer have a $1 \times N$ grating array and a $N \times N$ grating array, respectively. By suitably choosing the diffracted angle and diffraction efficiency of every grating, similar diffraction will be performed repeatedly at every grating. Finally, $N \times N$ output beams are obtained.

Keywords: Optical interconnect, holographic grating

Module optique de sortance de 1 à $N \times N$ pour interconnexions optiques

Résumé. On présente un nouveau type de module optique de sortance de 1 à $N \times N$ pour interconnexions optiques basé sur la structure d'hologrammes en mode substrat et consistant en deux couches de matières de réseaux. La première couche et la seconde sont respectivement des matrices $1 \times N$ et $N \times N$. En choisissant convenablement l'angle de diffraction et l'efficacité de chaque réseau, on obtient une diffraction similaire pour chacun des réseaux, on obtient finalement $N \times N$ sorties.

Mots clés: Interconnexions optiques, réseau holographique

1. Introduction

The intrinsic limitations of the current generation of computers have led researchers to seriously consider a new computer architecture based on optical interconnects [1]. It has been widely agreed that optical interconnects represent a better choice for interconnecting different processors and memories whenever conventional electrical interconnects cannot fulfil the system requirements. Among the optical interconnect architectures demonstrated thus far, optical interconnects based on a two-dimensional waveguide array and free-space interconnections represent current technological trends [2–6]. Owing to such trends, some array optical fan-out modules [2–4] using holographic grating arrays have been presented. Although it is easy to introduce them into the optical systems, it is difficult to fabricate them because every grating has its own specific structure. Furthermore, the noises coming from the cross-talk effects of some multiplex holographic structures are not negligible.

Some papers [7–11] have reported that optical interconnects using substrate-mode holograms with dichromated gelatin (DCG) recording material have many merits such as easy fabrication, low cost, high diffraction efficiency, are easily used, etc. Based on the structure of substrate-mode holograms, a new type of 1-to-($N \times N$) optical fan-out module is proposed for optical interconnects. This module consists of two layers of holographic volume grating arrays, but every grating has the same structure. Hence, it is very easy to fabricate them without changing the optical set-up for exposure. Besides this, it has the merits of conventional substrate-mode holograms [12], it can be applied to many optical signal processing systems by suitably choosing the diffraction efficiency, diffraction angle and the thickness of substrate.

2. Principle

The architecture of this new type of 1-to-($N \times N$) optical fan-out module which consists of two layers

0150-536X/97/020070+04$19.50

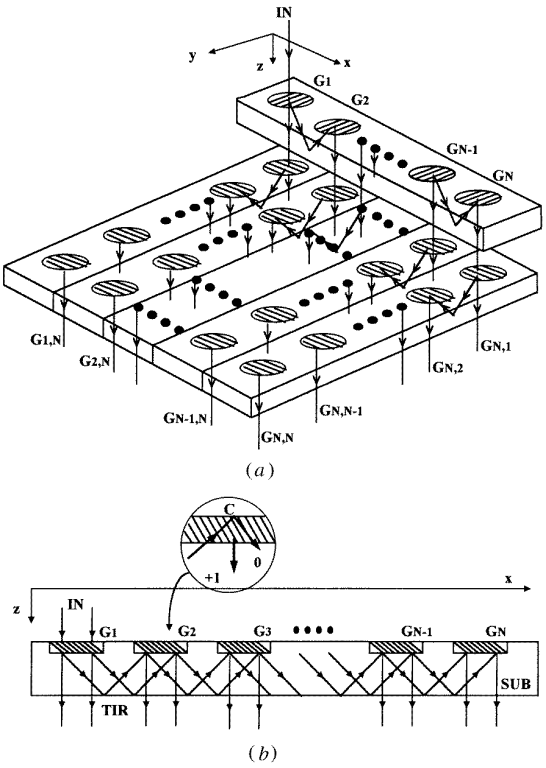

Figure 1. The architectures of (*a*) this 1-to-($N \times N$) optical fan-out module, and (*b*) of the $1 \times N$ grating array in the first layer.

of transmission-type volume grating arrays is shown in figure 1(*a*). The first layer has the $1 \times N$ grating array shown in figure 1(*b*). These N gratings have the same structure, the amplitude of the refractive index modulation of every grating is different so that every grating has its own specific coupling efficiency. The input beam of s-polarization is normally incident on the grating G_1, and it can be diffracted and divided into two parts: the zero-order diffracted beam and the first-order diffracted beam. The former is forward transmitted through the substrate without changing its direction and becomes one output of the first layer. On the other hand, the diffraction angle is designed so that it is larger than the critical angle in the substrate; therefore, the first-order diffracted beam propagates in the substrate as a form of guided wave until it arrives at G_2. This beam is again totally reflected at the interface, C, and its propagation direction is in parallel to that of the first-order diffracted beam coming from G_1. Because the structure of G_2 is the same as that of G_1, the first-order diffracted beam of G_2 will be parallel to the original input beam, that is, it passes normally through the substrate and becomes another output of the first layer. The detail of the wave-propagation in G_2 is shown in the circle inset of figure 1(*b*), and the zero-order diffracted beam continues its propagation in the substrate until it arrives at another grating, G_3. Because every grating has the same structure, the same diffraction performed at G_2 will be performed at $G_3, G_4, \ldots, G_N$. Hence, there are N output beams coming from the first layer. In order to equalize the intensities of these N output beams, the diffraction efficiencies of G_1, G_2, $G_3, \ldots, G_{N-1}$, and G_N should be $(N-1)/N$, $1/(N-1)$, $1/(N-2), \ldots, \frac{1}{2}$, and 1, respectively. The output beams of the first layer act as the input beams of the second layer.

The second layer has a $N \times N$ grating array which consists of N identical columns of $N \times 1$ grating arrays. Every column fans out the corresponding input beam into N output beams as performed by the first layer, but the propagation direction of a light beam in every column of this second layer is perpendicular to that in the first layer. The input beam is s-polarization for the first layer and is p-polarization for every column of the second layer, so every column is designed to have the same performance for p-polarization as that of the first layer for s-polarization. So, every grating of the second layer has the same structure as that of the grating in the first layer, but their grating vectors projected in the xy plane are orthogonal. Because similar diffraction conditions as those in the first layer are operated in every column of the second layer, the diffraction efficiencies of grating arrays of every column should be the same as those of the first layer, that is, they are $(N-1)/N$, $1/(N-1)$, $1/(N-2), \ldots, \frac{1}{2}$ and 1, respectively. Finally, $N \times N$ parallel output beams with equal intensity are obtained. Then, three main factors that strongly influence the performances of this new type of 1-to-($N \times N$) optical fan-out module will be discussed as follows. They are the diffraction efficiency, the fan-out packaging density and the optical path difference.

2.1. Diffraction efficiency of a volume grating

If d is the grating thickness, λ_r is the wavelength of the incident wave in free space, n_1 is the amplitude of the refractive index modulation, and θ_d is the diffraction angle in the phase volume grating, then the diffraction efficiencies of a transmission-type volume grating, for s- and p-polarizations under the Bragg condition can be written as [13]

$$\eta_s = \sin^2 \frac{\pi n_1 d}{\lambda_r \sqrt{\cos\theta_d}} \tag{1}$$

and

$$\eta_p = \sin^2 \frac{\pi n_1 d \sqrt{\cos\theta_d}}{\lambda_r} \tag{2}$$

respectively. Substituting the latter experimental conditions for a 5×5 fan-out module, $\lambda_r = 632.8$ nm, $d = 17$ μm and $\theta_d = 45^\circ$ into these two equations, we can get the relation curves of diffraction efficiency versus the amplitude of the refractive index modulation as shown in figure 2. Based on the relation curves shown in figure 2, the amplitudes of the refractive-index modulation of the grating arrays of the first layer are 0.0123, 0.0058, 0.0068, 0.0087, and 0.018, respectively; those for every column of the second layer are 0.001 74, 0.0082, 0.009 65, 0.0123, and 0.023, respectively. These amplitudes of the refractive-index modulation can be achieved with a suitable exposure time.

2.2. Fan-out packaging density

The fan-out spacing is determined by diffraction angle θ_d and the thickness of the first and second substrates. If the

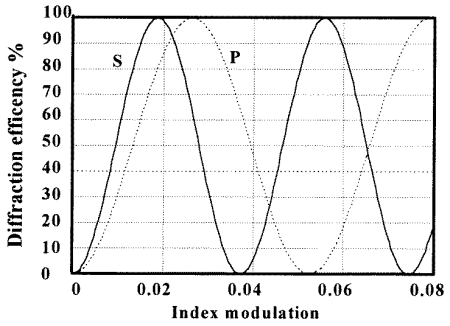

Figure 2. The calculated diffraction efficiency of a transmission volume grating versus the amplitude of the refractive index modulation.

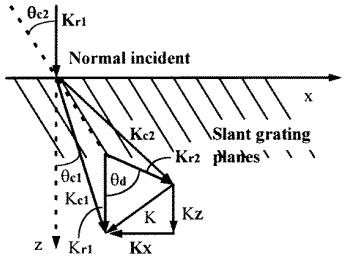

Figure 3. The *K*-vector diagram of short wavelength recording for long wavelength reconstruction.

thickness of the first and second substrates are t_1 and t_2, then the separations between any two nearest fan-out beams in the x- and y-directions are

$$Dx = 2t_1 \tan\theta_d \tag{3}$$

and

$$Dy = 2t_2 \tan\theta_d \tag{4}$$

respectively. Hence, θ_d, t_1, and t_2 should be chosen for the requirements of different systems with different fan-out spacings.

2.3. Optical path difference

As it is applied to an optical clock distribution system, the distributed optical path difference between the outputs of G_{11} and G_{ij} is

$$\Delta = 2(i-1)n_g t_1 \tan\theta_d + 2(j-1)n_g t_2 \tan\theta_d \tag{5}$$

where n_g is the refractive index of the substrate; and the corresponding time skew is $\tau_{ij} = \Delta/c$, where c is the velocity of light in a vacuum. For avoiding a serious clock skew, τ_{ij} must meet the requirements for signal synchronization.

3. Fabrication and results

In this paper, a 1-to-(5 × 5) optical fan-out module for 632.8 nm was given as an example. The photographic plate was obtained by coating the self-made DCG recording material onto BK7 glass. The thickness of the emulsion was

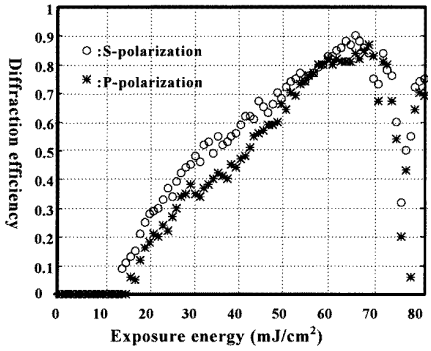

Figure 4. Experimentally measured diffraction efficiency versus exposure energy for a transmission grating made of DCG under the condition λ_c = 441.6 nm, λ_r = 632.8 nm, $\theta_d = 45^\circ$ and d = 17 μm.

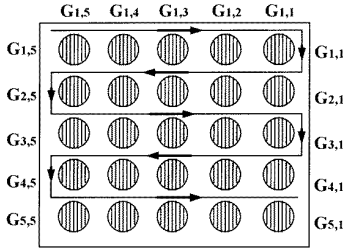

Figure 5. The fabricating order of every grating on the second layer.

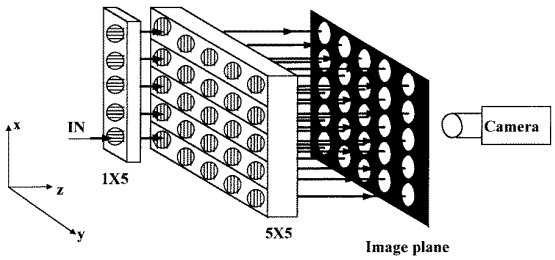

Figure 6. Optical set-up for demonstrating the performance of this module.

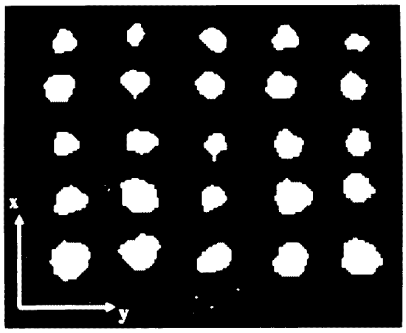

Figure 7. The photograph of the image of 5 × 5 output beams of this module.

17 μm. A He–Cd laser with 441.6 nm was used for fabricating this module and the recording geometry of two interfering beams can be determined with the *K*-vector diagram shown in figure 3. In this figure, K_{r1} and K_{r2} are the

wavevectors of the reconstruction wave and the diffracted wave, respectively at a wavelength $\lambda_r = 632.8$ nm, and K_{c1} and K_{c2} are the wavevectors of the construction reference wave and the object wave, respectively at a wavelength $\lambda_c = 441.6$ nm. From these geometrical relations, $\theta_{c1} = 7^\circ$ and $\theta_{c2} = 38^\circ$ are obtained, that is, 10.8° and 71° in free space, respectively; and a digital controlled high-precision pulse-translation system (model number PS-60X and CPC-3DN), manufactured by Japan Chuo Precision Industrial Co Ltd, was introduced into the optical set-up to displace the photographic plate during the exposure procedure. First, a series of gratings with different exposures was fabricated to investigate the real relation between the diffraction efficiency and the exposure energy and its experimental results are shown in figure 4. According to this figure, the exposure time corresponding to every grating could be estimated by the light intensity incident on the photographic plate. Next, the grating arrays of each layer are fabricated with moderate exposure. For convenience, the grating arrays of the second layer were fabricated according to the order shown by figure 5. The gratings on the same rows were fabricated with the same exposure, the gratings on the different rows were fabricated with different exposures. The real diffraction efficiencies of $G_1 \sim G_5$ on the first layer are 80, 26, 33, 52, and 89%, respectively and the real diffraction efficiencies of $G_{1,N} \sim G_{5,N}$ ($N = 1, \ldots, 5$) of every column on the second layer are 80, 24, 34, 49 and 90%, respectively. Then, the first layer was superposed on the second layer accurately and a 1-to-(5×5) fan-out module was obtained. The substrate thicknesses of two layers are 9 and 20 mm, respectively, and the size of this module is $100 \times 200 \times 30$ mm. In order to see its performance, the module was performed with the set-up shown in figure 6, in which a piece of ground glass was used for the image plane and a camera was focused on this plane. Figure 7 shows the images of 5×5 output beams. The diameter of the input beam is about 4 mm, and the output separations along x- and y-directions are about 20 and 42 mm, respectively. The total efficiency of this module is 89%.

4. Discussion

The input beam and the output beams are parallel and perpendicular to this module, and it is very easy to introduce this module into optical systems. The module for s-polarization input is derived, and the module for p-polarization input can be designed and fabricated similarly.

Both the scattering at each boundary where the light beam is totally internally reflected and the fringe shrinkage in photographic emulsion during chemical processing will strongly influence the output qualities and the diffracted angle. These drawbacks are more obvious as the numbers of total internal reflections increase, and they could blur the images of the output beams and make the output-beam intensities non-uniform. In order to reduce the scattering at each boundary, the surface of the guiding substrate should be clean, and fringe shrinkage can be compensated by the appropriate process and estimation [14].

As this module is integrated into a practical system, both the size of this module and the polarization of the output beams should be considered. Its size should be suitably chosen to match the real requirement of the system without introducing serious clock skews.

5. Conclusion

Based on the structures of substrate-mode holograms, a new type of 1-to-($N \times N$) optical fan-out module is proposed for optical interconnects. Optimum design rules are provided with experimental results. This new interconnection scheme has one-to-many and many-to-many parallel fan-out capabilities, by using a light-guiding plate integrated with a two-dimensional holographic volume grating array made out of DCG film. Such an interconnection scheme is applicable to a myriad of large-scale multi-stage optical intra- and inter-board fan-out applications.

Acknowledgment

This study was supported by the National Science Council, Taiwan, Republic of China, under contract number NSC85-2215-E-009-011.

References

[1] Goodman J W, Leonberger F L I, Kung S and Athale R A 1984 Optical interconnections for VLSI systems *Proc. IEEE* **72** 850–66

[2] Tang S and Chen R T 1994 1-to-27 highly parallel three-dimensional intra- and inter-board optical interconnects *IEEE Phot. Technol. Lett.* **6** 299–301

[3] Tang S and Chen R T 1994 1-to-42 optoelectronic interconnection for intra-multichip-module clock signal distribution *Appl. Phys. Lett.* **64** 2931–3

[4] Wang M R, Sonek G J, Chen R J and Jannson T 1992 Large fanout optical interconnects using thick holographic gratings and substrate wave propagation *Appl. Opt.* **31** 236–49

[5] Walker S J and Jahns J 1992 Optical clock distribution using integrated free-space optics *Opt. Commun.* **90** 359–71

[6] Bergman L A, Wu W H, Jahnston A R, Nixon R, Esener S C, Guest C C, Yu P, Drabik T J, Feldman M and Lee S H 1986 Holographic optical interconnects for VLSI *Opt. Eng.* **25** 1109–18

[7] Kostuk R K, Kato M and Huang Y T 1990 Polarization properties of substrate-mode holographic interconnects *Appl. Opt.* **29** 3848–54

[8] Yeh J H and Kostuk R K 1995 Substrate-mode holograms used in optical interconnects: design issues *Appl. Opt.* **34** 3152–64

[9] Govindarajan M and Forrest S R 1991 Optically powered arrays for optoelectronic interconnection networks *Appl. Opt.* **30** 1335–46

[10] Chen R T, Wang M R and Jannson T 1990 Intraplane guided wave massive fanout optical interconnections *Appl. Phys. Lett.* **57** 2071–3

[11] Parker J W 1991 Optical interconnection for advance processor system: a review of the ESPRIT II OLIVES program *J. Light. Technol.* **9** 1764–993

[12] Kostuk R K, Huang Y T, Hetherington D and Kato M 1989 Reducing alignment and chromatic sensitivity of holographic optical interconnects with substrate-mode holograms *Appl. Opt.* **28** 4939–44

[13] Kogelnik H 1969 Coupled wave theory for thick hologram gratings *Bell Sys. Technol. J.* **48** 2909–47

[14] Chang B J 1980 Dichromated gelatin holograms and their applications *Opt. Eng.* **19** 642–8